CHAPTER 28

Langmuir–Blodgett Films

Hubert Motschmann and Helmuth Möhwald

Max-Planck-Institute of Colloids and Interfaces, Golm, Germany

1 LANGMUIR–BLODGETT FILMS

In the 1980s, there was great enthusiasm about molecular assemblies based on Langmuir–Blodgett (LB) films. Visions were proposed for the next millennium such as "Molecular electronics in which organic molecules perform an active function in the processing of information and in transmission and storage" (1–3). These proposals raised many expectations. Being now at the beginning of a new millennium, this review will aim to critically assess the accomplishments and perspectives. This present chapter will cover applications, as well as some fundamental experiments in which LB films have served as model surfaces to study interactions. The selection is somewhat personal since it is not possible to give this whole field full coverage on account of space restrictions. This chapter covers conventional LB films, as well as novel new types obtained by the organization of nanoparticles at the air–water interface. The LB technique extended to this class of materials allows the fabrication of ordered arrays of quantum dots of semiconductor, metal or insulator particles, and provides a convenient handle on decisive parameters such as the inter-particle spacing. LB films possess a high orientational order, and for this reason, an inherent potential for nonlinear optical devices such as frequency doublers or modulators. We will discuss in detail selected nonlinear optical devices where the control of the internal layer structure on a molecular level was utilized for maximization of the efficiency. These assemblies operate close to a practical level of performance, but face a strong competition with alternative approaches and technologies. Another promising application is the field of sensing and we will report on recent advances in the design of gas sensors. We will report also on some exciting new achievements which are far away from practical utilization, such as the molecular rectifier or the design of command surfaces where a single photoactive moiety may be sufficient to determine the orientation of a bulk liquid crystal.

1.1   What makes LB films appealing?

The appealing features of Langmuir–Blodgett films is the intrinsic control of the internal layer structure down to a molecular level and the precise control of the resulting film thickness. Sophisticated LB troughs allow us to process several materials with different functionalities and offer the possibility to tune the layer architecture according to the demands of the desired molecularly engineered organic thin-film devices. It is worthwhile to start this review with a brief consideration of the fabrication process. Further details can be found in the books by Gaines (4) or Ulman (5); the latter also presents a good introduction to the surface analytical tools which are commonly used for the investigation of the structure of monolayers and various physical properties.

The first step of the LB deposition process is the formation of a well defined monolayer at the air–water interface. These so-called Langmuir monolayers are a precursor film within the LB fabrication. The preparation process is illustrated schematically in Figure 28.1. The amphiphile is dissolved in an organic solvent and subsequently spread at the air–water interface. The solvent evaporates and a monolayer of the amphiphile at the air–water interface is then produced. These Langmuir monolayers can be further manipulated by means of a moveable barrier which allows us to control the area per molecule. Monolayers at the air–water interface have been extensively studied and possess a richness of phases and structures. They serve as quasi-two-dimensional model systems and have thus attracted a significant amount of research effort. The advent of sophisticated surface analytical tools such as X-ray reflection and scattering techniques, together with novel optical techniques such as the Fluorescence and Brewster Angle Microscopy (BAM), have provided a detailed picture of the general phase diagrams, structure and morphology. Grazing-Incidence X-ray diffraction has revealed the existence of several phases in which the aliphatic chain is tilted with respect to the surface normal and in which the tilt azimuth adopts a well-defined arrangement with respect to the underlying bond orientational order (6). The organization of the tilt azimuth can extend to macroscopic dimensions and thus shows up in BAM images in various facets such as the formation of domains with an internal structure. The review articles of Möhwald (7), McConnel (8), Knobler and Desai (9), Riviere *et al.* (10) and Knobler and Schwartz (11) are excellent guides through the vast amount of publications covering the field of Langmuir monolayers.

The Langmuir–Blodgett technique utilizes these monolayers as building blocks for the fabrication of thin layers by transferring the Langmuir monolayer on to a solid support. The deposition process is controlled by the hydrophilicity or hydrophobicity of the solid support. A monolayer at the air–water interface can be transferred by an up-stroke on to a hydrophilic surface (see Figure 28.1(c)) and via a down-stroke on to a hydrophobic surface. Several trough designs have been proposed and there are also commercially available multi-compartment troughs which allow the simultaneous processing of different materials (as shown in Figure 28.1(d)). In this figure, compartment A contains a different material to compartment B. Both monolayers can be independently compressed to their target pressure and the dipping robotic control is programmed for the desired dipping sequence which determines the layer architecture on the molecular level, as well as the upside-down orientation of the molecule (Figure 28.1(e)). Many applications, such as nonlinear optical devices, require a stacking of the molecules in a predefined arrangement with a high orientational order. LB films possess an inherent potential for such applications. However, unfortunately molecules quite frequently do not behave in the way that they are depicted in simple schematics and the deposition process actually turns out to be a fairly complex process governed by many parameters such as surface viscosity, surface energies, hydrodynamic flow and water drainage. It is therefore worthwhile to consider the deposition process in a bit closer detail.

1.2   Details of the deposition process

The deposition is usually monitored by the corresponding transfer ratio. During monolayer transfer, a further compression is required in order to maintain a constant surface pressure. The transfer ratio is defined as the ratio of the decrease in Langmuir monolayer surface area divided by the area of the solid support which has been coated. The user tries to adjust the experimental conditions such as the transfer speed, temperature and sub-phase composition (e.g. indifferent electrolytes) such that a transfer ratio close to one is achieved. The underlying assumption is that the Langmuir monolayer then serves as a simple building block which resembles the features of the pre-formed monolayer at the air–water interface. Repeated dipping cycles simply provide replicas of the monolayer and such monolayers thus allow the formation of stratified layer structures in the same manner as bricks are used to set up a wall in the

(a)

(b)

(c)

(d)

Side A

Side B

(e)
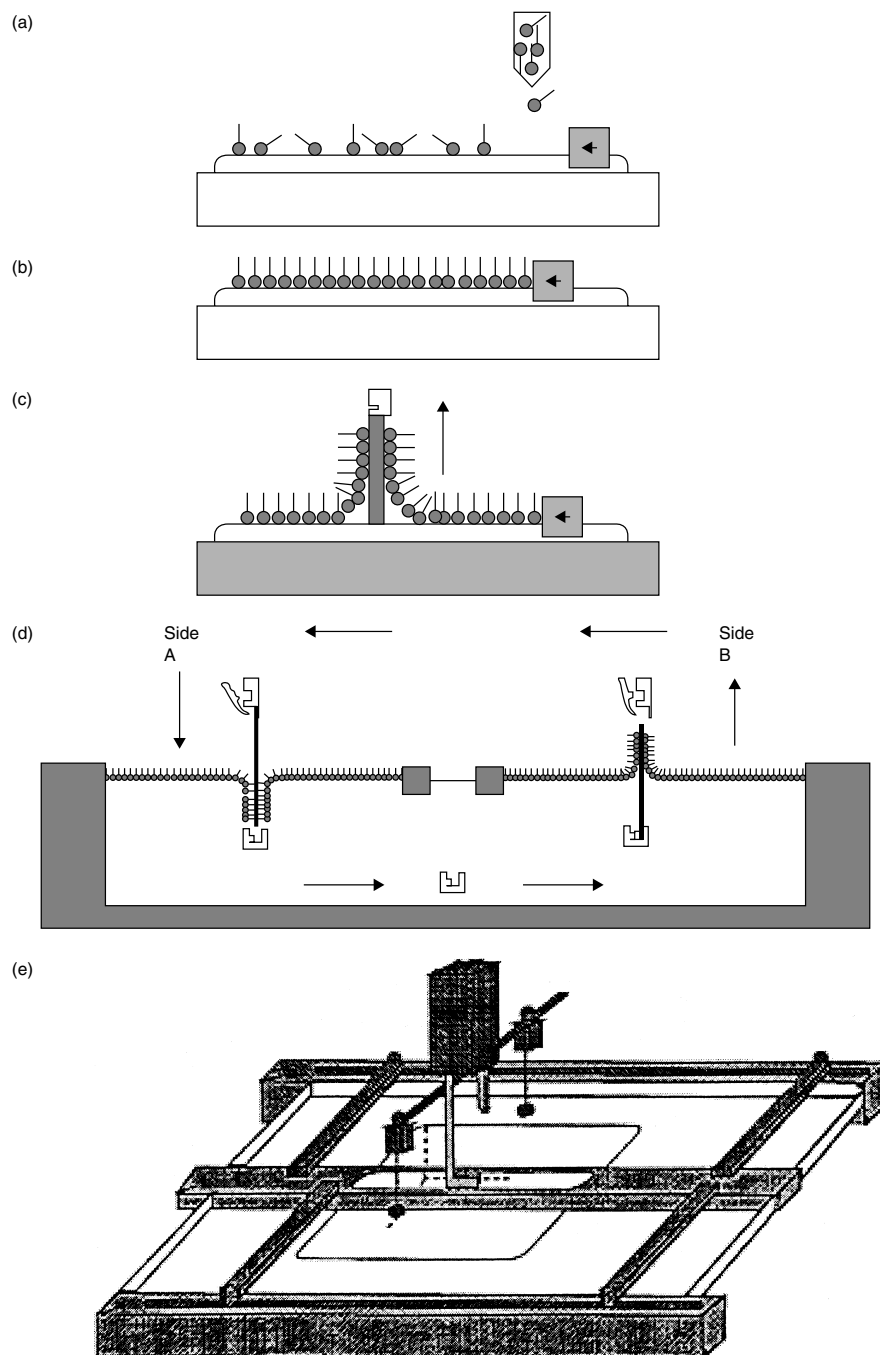
Figure 28.1. Schematic of the Langmuir−Blogett deposition process. The amphiphile is dissolved in an organic solvent and subsequently spread at the air−water interface. The solvent evaporates and a monolayer of the amphiphile at the air−water interface remains (a). The monolayer at the air−water interface can be further manipulated by means of a movable barrier allowing control of the area per molecule (b). The Langmuir monolayer can be transferred by an up-stroke on to a hydrophilic surface (c) and via a down-stroke on to a hydrophobic surface. A dual compartment trough enables the simultaneous processing of two different materials (d), while a programmed dipping sequence allows the determination of layer architecture at a molecular level

macroscopic world. However, the difference in the local environment on a solid support and at the air–water interface may give rise to certain structural changes. The transfer requires a drainage of the film and the monolayer properties will also be partly governed by the hydrodynamic flow during the transfer. The film may reorganize and there is a high chance that the deposited film may not reach its local thermodynamic minimum and remains instead in a non-equilibrium state. The transfer is the crucial step within the LB technique and many experimental groups have addressed the relationship between the monolayer structure of the precursor film at the air–water interface and the one observed on a solid support. This is not a unique picture and there are examples where no changes are observed, as well as examples with strikingly different structures and features between the monolayers at the air–water interface and on the solid support.

Tippmann-Krayer *et al.* (12) have investigated the monolayer structure of cadmium arachidate at the air–water interface and on a hydrophilic support by using grazing incidence X-ray diffraction. In both cases, they observed a very similar hexagonal structure with the aliphatic chains oriented normal to the surface. Shih *et al.* (13) investigated the structure of fatty acid monolayers (heneicosanoic acid) transferred to glass substrates from three different phases of the monolayer at the air–water interface by also using grazing incidence X-ray diffraction. In all cases, the transferred films adopt the very same structure with an upright orientation and hexagonal packing, irrespective of the structure of the monolayer phase, even if the Langmuir monolayer adopts a distorted hexagonal packing in which the molecules are tilted towards their neighbours. Apparently, the upright hexagonal packing represents a local energety minimum of the hydrocarbon chains. Durbin *et al.* (14) have performed detailed *in situ* X-ray diffraction studies of the deposition process. The experimental set-up allowed an investigation of the Langmuir monolayer as well as the freshly prepared LB film in the same closed temperature-controlled environment. Monolayers of fatty acids have been deposited from three different phases. In all cases, the very same structure was also observed on the solid support immediately after the deposition. The monolayer survived the transfer; however, these authors report on some structural changes occurring long after deposition as a result of the drying process. The data suggest the possibility of preserving the structure of the Langmuir layer provided that the heating and drying condition are carefully adjusted. Gehlert *et al.* (15) demonstrated that domains of condensed monolayer phases can be transferred on to a solid support without any changes in morphology. The domains of a condensed phase of certain glycerol esters possess a "star texture" which is the result of a tilt organization on a macroscopic scale. The same tilt organization was found on a solid support. In a beautiful experiment, these layers have been used as command layers which determine the anchoring and orientation of the bulk phase of nematic liquid crystals (16). A conventional microscope is then sufficient to visualize the texture, as shown in Figure 28.2.

During LB deposition, remarkable phenomenon such as wetting instabilities may occur which show up in the formation of regular stripes on the support (17). The underlying mechanism is likely to be caused by a feedback between the meniscus height, as determined by the contact angle, and changes in the work of adhesion at the substrate, caused by changes in the packing density within the monolayer (18). The static meniscus height is governed by the surface tension and is higher than the planar water surface. The transfer on to the solid support is determined by the prevailing interaction of amphiphile and solid surface. A strong interaction leads
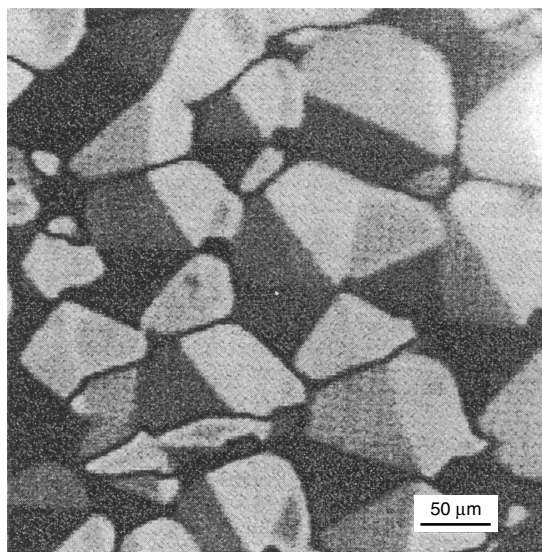
Figure 28.2. Monolayers of the amphiphile 1-monopalmitoyl-(±)-glycerol at the air–water interface assemble in domains in which the molecular tilt azimuth is organized in "star-shaped" patterns. It is possible to preserve this order during the transfer on to a solid support. LB monolayers of this material have been utilized for the anchoring of nematic liquid crystals. The order within the monolayer determines the order within the bulk phase of the nematic liquid crystal (LC). The image here shows the LC cell between crossed polarizers. (From J. Fang, U. Gehlert, R. Shashidar and C. Knobler, *Langmuir* (1999), **15**, 297)

to a rapid adherence of the molecules, which in turn reduces the surface energy and leads to an increase in the contact angle, as described by Young's equation (19). As a consequence, the meniscus height decreases. On the other hand, the meniscus height will tend to exceed its equilibrium height during the continuous up-stroke movement of the solid support, hence leading to an accelerated adsorption. Thus, the dynamic behaviour of the meniscus is governed by two counteracting processes which show up in an oscillation of the meniscus. Gleiche and Chi. (20) demonstrated recently that it is possible to obtain quite regularly spaced stripes with channels of a size of 200–300 nm, as shown in Figure 28.3.
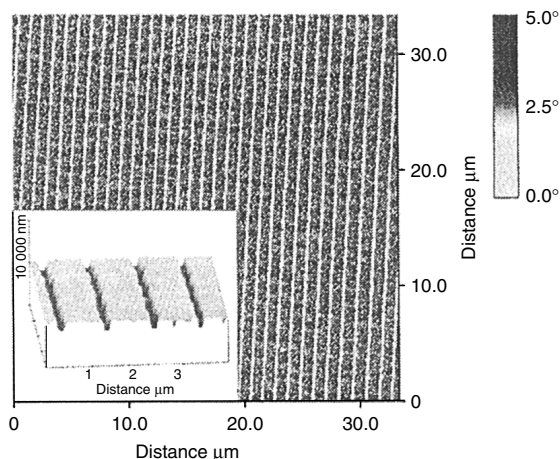
1.3 New types of LB films based on nanoparticles

The fabrication of size-quantized semiconductor and metal nanoparticles has attracted a lot of attention (21–23) because of their novel optical and electrical properties and their appealing features as models for basic science. The LB deposition process originally developed for amphiphiles can also be extended

Figure 28.3. Dipalmitoyl phosphatidylcholine (DPPC) transferred on to a solid support at a rather high transfer speed of 1000 µm/s at a lateral surface pressure of 3.0 mN/m^{-1}. Dynamic scanning force microscopy (SFM) images provide evidence for the formation of a regularly structured surface, revealing channels with a width of about 200 nm separated by 800 nm wide stripes of the monomolecular film. The main figure represents phase and and the inset (4 × 4 µm^2) topography imaging. The monolayer was prepared on pure water at room temperature; A change in the temperature influences the periodicity. (From M. Gleiche and L. F. Chi), *Nature*, **403**, 2000, 173)

to nanoparticles. It has been demonstrated that properly coated nanoparticles can be organized at the air–water interface by using a similar procedure to that illustrated in Figure 28.1. The corresponding films possess striking similarities to those observed for classical Langmuir monolayers. The coating of the nanoparticle is a decisive factor in the ability of such particles to form monolayers with well-defined π, A-isotherms. Once the hydrophobicity is too low the particles sinks, whereas the particles tend to stick to unwanted aggregates if the coating is too hydrophobic. Fendler and co-workers have demonstrated that a variety of different metal or metal oxide particles can be properly coated and processed at the air–water interface, e.g. cadmium sulfide (24), titanium dioxide (25, 26), magnetic iron oxide (27), and several noble metal particles (28, 29). It was further demonstrated that the films of nanosized particles at the air–water interface can also be transferred on to a solid support by using the established standard LB dipping technique or the horizontal lifting techniques originally developed by Langmuir and Schäfer (30). In many cases, a transfer ratio close to one could be achieved. In addition, experimental evidence has been provided that the layer thickness of properly designed systems changes in a linear fashion with the number of deposited layer, thus allowinging the fabrication of rather complex superlattices of different particles.

Heath *et al*. have (31) investigated in great detail the pressure/temperature phase diagrams of organically passivated Ag and Au nanocrystals with diameters of 20–75 Å. The particles were self-assembled at the air–water interface and the structures of the observed phases were investigated by transmission electron microscopy of the corresponding Langmuir–Blodgett films. The roles of particle size, size distribution and the size of the passivating organic ligand were addressed. The features could be categorized according to the excess volume available to the ligand as it extends from the surface of the particle. At large excess volumes, low-density structures with chain and ring morphologies are observed, while at higher surface pressures foam-like phases which can be further compressed into a two-dimensional closed packing are seen, before a transition to irreversible non-equilibrium structure is observed. The crystalline order within the close-packed phase is limited by the width of the particle distribution.

The appealing feature offered by the LB deposition of nanoparticles is the possibility to generate ordered arrays of metal quantum dots with new features due to the prevailing confinement. The band gap of a semiconductor nanoparticle is strongly size-dependent, while the optical absorption of metal nanoparticles depends on

size and inter-particulate spacing. The LB technique and the choice of the passivating organic layer provides a handle on the latter and allows tuning of the electronic properties. Heath and co-workers have measured the linear and nonlinear responses of several monodisperse Ag particles with a diameter of 2–7 nm, capped by alkanethiols of different chain lengths (32). The metal dots were organized at the air–water interface and the optical properties were monitored as a function of the interparticle distance. At a latter distance of less than 5 Å, the second-harmonic generation (SHG) response exhibits a sharp discontinuity and the linear reflectance and adsorbance resembles the features of thin metal films, thus indicating an insulator-to-metal transition (32). The linear response is dominated by the surface plasmon resonance, ω_{sp}, which resembles the physical dimensions of the particle (33). At lower inter-particle distances, the dielectric medium in between the particles is modified by the presence of the conducting spheres and a quantum mechanical coupling occurs which allows a delocalization of charge carriers over several particles. As a result, the plasmon resonance shifts to lower values which resemble the features of thin metal films in the case of a complete delocalization. Direct evidence for a reversible metal–insulator transition was provided by impedance spectroscopy measurements on the same system (34). With compression of the nanocrystal monolayer, the complex impedance of the films undergoes a transition from a parallel resistance-capacitance (RC) equivalent circuit to an inductive circuit. At large particle distances the particles maintain their individual electronic identity and the film is insulating, while it resembles the features of a thin metal at higher coverage. Meanwhile, four different electronic signatures have been identified within thin assemblies of metallic nanocrystals, which depend on the inter-particle distance and the order within the film (35). The investigation of these systems also provides an insight into the impact of disorder in superlattices of nanocrystals on the corresponding electronic properties. An understanding of the underlying relation ships thus allows us to deliberately tune the electronic properties.
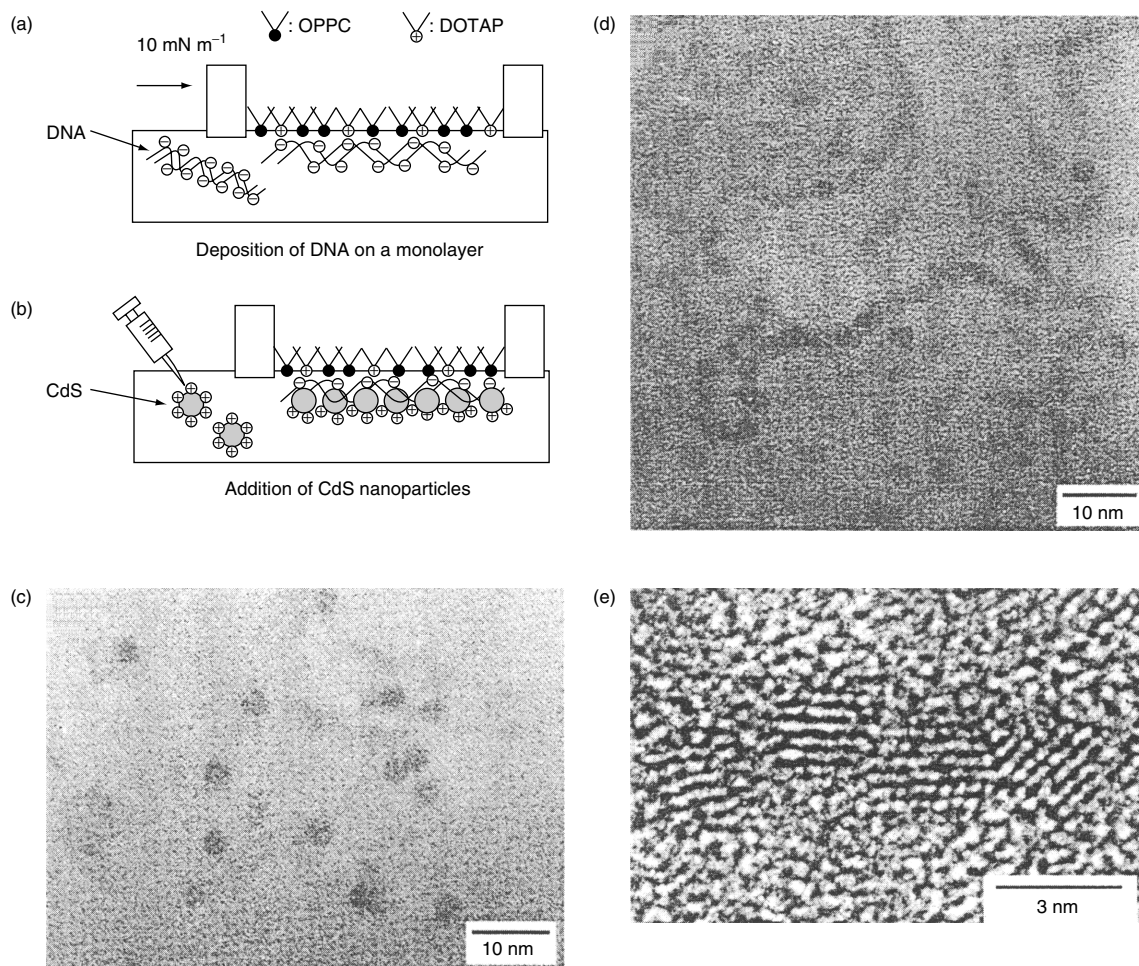
Similar studies have been carried out for monodisperse magnetic particles deposited on water surfaces (36). The resulting structures are the result of a balance between van der Waals and magnetic dipole–dipole interactions.

The detailed knowledge gained in the last few decades about the organization of amphiphiles at the air–water interface can also be utilized for the design of proper templates for the organization of nanoparticles. A nice example was recently given by Torimoto *et al.* (37).

A Langmuir monolayer of a mixture of the cationic amphiphile alkyltrimethylammoniumpropane (DOTAP) and a phospholipid (OPPC) was prepared and compressed to a defined state. The Langmuir monolayer possesses a positive net charge, and DNA double strands injected in the sub-phase readily adsorb at the interface due to the electrostatic attraction between the phosphate groups of the DNA and the quaternary ammonium groups of DOTAP (see Figure 28.4(a)). This performed assembly was then exposed to a very dilute solution of positively charged CdS particles. These particles adsorb and are immobilized along the DNA strands due to the prevailing electrostatic interaction (Figure 28.4(b)). The assembly was transferred on to an electron microscope grid and characterized by using transmission electron microscopy. The images reveals a dense packing of the nanoparticles along the DNA strand, with a line width equal to the diameter of a particle. Figures 28.4(c–e) shows the corresponding images.

1.4 Summary

At this stage, the reader should be aware that the transfer process is governed by many parameters and the adopted structure is the result of a subtle interplay of various interactions. A transfer ratio of one does not mean that Langmuir layer and deposited layer will adopt an identical structure. This may hold, although the corresponding structures can also be completely different. The probability for structural changes during the deposition is linked to the rigidity of the system. Structural changes are more likely to occur in less rigid structures which are fairly sensitive to details of the local environment. Rigid structures lack this sensitivity, and hence structural changes with deposition are less likely to occur. However, it is extremely difficult to work out proper deposition conditions for stiff systems and LB films of such materials commonly exhibit a fairly high number of defects such as domains or grain boundaries. The way out of this apparent dilemma is opened up by using polymeric LB layers which form fairly smooth and defect-free films. Usually, LB layers of polymeric materials are fairly insensitive to the local environment and can be transferred on to a solid support with little or no changes when compared to the precursor film at the air–water interface. The structure adopted at the solid support may also be frozen in a non-equilibrium state and not in its local energetic minimum. This may also be the reason for some contradictions between findings within different laboratories. Further details can be found in the article by Schwartz (38). The utilization

(a) 10 mN m^{-1}

∨: OPPC ∨: DOTAP

DNA

Deposition of DNA on a monolayer

(b)

CdS

Addition of CdS nanoparticles

(d)

10 nm

(c)

10 nm

(e)

3 nm

Figure 28.4. A mixed monolayer of a cationic amphiphile DOTAP and a phospholipid (OPPC) was prepared at the air–water interface. DNA readily adsorbs at the monolayer due to the electrostatic interaction (a). CdS nanoparticles can then organize as a chain along the DNA strands (b), as revealed in the TEM images (c–e). (From T. Torimoto, M. Yamashita, S. Kuwabata, T. Sakata, H. Mori and H. Yoneyama, The Journal of Physical Chemistry B; (1999) **103(42)**; 8799)

of the LB technique requires a careful choice of *all* parameters which can unfortunately be rather a tedious enterprise.

Several attempts were undertaken to modify the trough instrumentation in order to upgrade the LB deposition from laboratory scale to one of an industrial pilot project, which required a complete automatization of all of the underlying procedures. The troughs in this case are completely different to conventional troughs with moving barriers, and utilize instead the stress generated by a flowing sub-phase for the compression of the monolayer (39). The results reported by O. Albrecht *et al.* at Canon (40) are encouraging, showing that it is

indeed possible to bring LB technology to a state that is compatible with the necessary reliability, throughput and quality for mass production provided that all parameters are well adjusted.

2 MOLECULAR ASSEMBLIES WITH FUNCTIONS

Two applications have been earlier identified where LB films might have great potential, namely nonlinear optical devices based on a second-order effect, and sensors. The research on these topics is quite advanced

and at the present time there are thin-film assemblies available which are already close to a practical level of performance. One of the long-term goals is application as molecular electronic devices, which is discussed in the Section 2.4 below.

2.1 Nonlinear optical devices based on second-order effects

2.1.1 Background

Nonlinear optical (NLO) effects are the result of the interaction of intense laser light with matter. The electric field strength generated by an intense laser pulse is comparable to the inner atomic electric fields. As a result, the electric field induces a nonlinear polarization. The nonlinear interaction gives rise to two fascinating effects not known in linear optics, namely photons can be split into two parts or can be merged together. A sound introduction to this field can be found in the texts by Boyd (41) or Shen (42). Facets of the prevailing nonlinearity are the generation of new frequencies such as in frequency-doubling or sum-frequency generation, the modulation of light by an external electric or magnetic field via the Pockels or Faraday effects, or the possibility to influence "light with light", which is the major hurdle towards all-optical signal processing. Several photonic devices have been proposed which exploit and utilize these effects. For the scope of this present review, a brief phenomenological treatment is sufficient in order to introduce some basic terms and equations and familiarize the reader with some device concepts. The interaction between the external electric field $\mathbf{E}$ and the resulting polarization $\mathbf{P}$ is nonlinear and can be represented as a power series, as follows:

$$\mathbf{P} = \varepsilon_0(\chi^{(1)}\mathbf{E} + \chi^{(2)}\mathbf{EE} + \chi^{(3)}\mathbf{EEE} + \cdots) \qquad (28.1)$$

A propagating electromagnetic wave is accompanied by a nonlinear polarization wave which in turn may act as a source term for radiation at new frequencies. This is used for an extension of the frequency range of laser light sources (43). All effects of the second-order are governed by the quadratic term in $\mathbf{E}$ and the utilization requires a maximization of the magnitude of the macroscopic susceptibility tensor of the second-order, $\chi^{(2)}$. The relation of $\chi^{(2)}$ with the corresponding molecular quantities is provided by the oriented gas model, which successfully describes, despite certain simplifying assumptions, thin film assemblies of organic molecules as follows:

$$\chi^{(2)} \propto \sum_{\text{molecules}} \beta \propto N\langle\beta\rangle \qquad (28.2)$$

Equation (28.2) states that the macroscopic susceptibility $\chi^{(2)}$ is proportional to the sum of all hyperpolarizabilities β of all molecules, where β is the molecular pendent to $\chi^{(2)}$ and relates the induced dipole moment with the quadratic term of the local field acting on the molecule. This can alternatively be expressed by the number density N of the active unit and the orientational average of β (as denoted by the angular brackets). Obviously, $\chi^{(2)}$ vanishes if the molecules adopt a centrosymmetric arrangement, even if the molecules possess a high β. Equation (28.2) outlines the requirements for structures with a high $\chi^{(2)}$. Molecules with a high hyperpolarizability β should be arranged in a non-centrosymmetric fashion with a high and uniform orientation. Furthermore, the number density of the active unit should be maximized.

Molecules with a high β have some structural elements in common. They all possess an extended π-system, further modified with groups "pushing" and "pulling" the electron density of the molecules (44–46). The π electrons provide the required high polarizability and the push pull system provides the noncentrosymmetry on a molecular scale which is required for a non vanishing hyperpolarizability β. Extremely high values of the effective hyperpolarizabilities have been reported for organic molecules (44, 47, 48) and these findings motivate further applied research. At present, the major obstacle towards efficient devices is not the availability of suitable chromophores, but the fabrication of a proper macroscopic structure which has to simultaneously meet many requirements, such as a high $\chi^{(2)}$, sufficient thermal and mechanical stabilities, and the possibility to enable phase-matching. Many of these issues will be discussed in the following. LB films have an inherent potential for these applications due to the intrinsic orientation order and the possibility to precisely tune the thickness and the internal layer structure.

2.1.2 Model systems

Organic molecules can be tailored according to specific demands and different desired functionalities can be incorporated within a single molecule (5, 44). In order to be able to process the material via the LB technique, the NLO chromophore has to be incorporated within an amphiphile. An unwanted side effect is the dilution of the active unit within the assembly. A

non-centrosymmetric arrangement further requires that the NLO active material is interleaved with compatible spacer materials. The fabrication requires a dual-compartment trough. The active unit is still assembled in an non-centrosymmetric fashion with a high orientation, while the deposition is still governed by the thermodynamically stable head–head and tail–tail arrangements between active and inactive material (see Figure 28.1).

A lot of research is still devoted to the identification and design of suitable model systems which meet the requirements imposed by both the LB technique and nonlinear optics. The focus of this work is the achievement of a uniform film with a high nonlinear susceptibility. Furthermore, the film quality should not degrade with the number of deposition cycles. An established and quite sensitive test relies on an investigation of the relation between the second-harmonic generation (SHG) intensity measured in reflection or transmission and the layer number. A quadratic dependence provides experimental evidence that the properties of the bilayer do not change with the deposition. Hence, a bilayer of NLO active material and spacer can be regarded as a simple building block for the design of complex molecular assemblies.

There are numerous investigations which address these issues, and many systems have been identified which fulfil these properties. Ashwell and co-workers have investigated two different systems which all exhibit the quadratic dependence and which do not show any signs of degradation during the deposition of many layers (49–52). The results obtained with a coumarine dye interleaved with an inert spacer dye are remarkable (53). These authors report an extremely high susceptibility of $\chi_{\text{eff}}^{(2)} = 190 \pm 30$ pm/C. This is the highest susceptibility reported to date. However, this value was measured under resonance enhancement and should be regarded with some scepticism. Non-centrosymmetry requires the processing of two materials and in most studies an active and an inactive material is used which leads to a unwanted dilution of the active unit. This problem was tackled in and reported in refs (54) and (55). Instead of using active and inactive materials, two different NLO chromophores were processed. The chromophore orientation in one amphiphile is upside-down with respect to that of the second amphiphile. Thus, the stable head-to-head and tail-to-tail configurations are still maintained while the chromophore adopts a uniform non-centrosymmetric arrangement. Both experiments used a polymeric material with the active unit in the side-chain. The model systems obeyed the oriented gas model and lead to a significant enhancement in the SHG efficiency as a result of the higher number density.

A new approach to second-order nonlinear materials was reported by Verbiest *et al.* (56) in which chirality plays the key role. These authors investigated Langmuir–Blodgett films of chiral helicenes which lack features commonly associated with a high SHG response. The molecules adopt a helical structure on a solid support and this chiral supramolecular arrangement enhances the second-order NLO susceptibility by a factor of 30 when compared to the corresponding racemic mixture. An adequate description of the SHG response in a chiral system requires additional tensor elements. Experimental evidence was provided that those tensor elements which are only allowed in a chiral environment dominate the SHG response of the helicene system.

To summarize these achievements – several model systems have been designed which allow the formation of fairly thick layers with a sufficiently high susceptibility to meet the requirement imposed by application. However, while there are still efforts aiming for the design of new model systems, the challenging task is now the integration of structures with a high $\chi^{(2)}$ in photonic devices.

2.1.3 Hyperpolarizabilty and adsorption trade-off

A discussion of many photonic devices can be found in the book by Prasad and Williams (44). Promising application are modulators which exploit the electro-optic effect or frequency doubler properties for an extension of the frequency range of laser light sources. In particular, high-efficiency converters capable of doubling the continuous-wave (CW) light of near-infrared laser diodes have a tremendous potential market. The advent of blue laser diodes is desirable in order to increase the storage density of optical storage devices. The storage density is linked to the wavelength of light used for "reading" and "writing" devices. A doubling of the frequency increases the storage capacity by a factor of four. This has motivated intense research in this field involving different strategies. One is the frequency doubling of cw-low-power laser diodes by using supramolecular organic structures and this also provides a nice example as to how a molecular assembly can perform new desired functions.

The figure of merit for all devices based on a second-order effect is given by the ratio of the susceptibility $\chi^{(2)}$ and refractive index n as $\chi^{(2)^2}/n^3$. Organic materials possess a lower refractive index ($n \approx 1.4-1.6$) than inorganic materials ($n \approx 2.2-3.5$), and this also gives them, in this respect, an edge over their inorganic counterparts.

All practical applications require the use of a waveguide format. An optical waveguide is a region with an elevated refractive index, and where the light is confined in one or two dimensions. The propagation of light can be described in the ray picture by total reflection. The light is propagating in well-defined modes characterized by a specific field distribution with several nodal planes. The waveguide format overcomes diffraction and allows the maintenance of high power over a long interaction length. The waveguide format is also compatible with other concepts of integrated optics (58) and several papers have successfully demonstrated the integration of organic films with semiconductors devices (59, 60). However, several complications are imposed from the need for a waveguide format. The thickness of a waveguide is comparable to the wavelength of light and hence the deposition of several hundreds of bilayers is required. Furthermore, the waveguide has to be transparent at all propagating wavelengths in order to prevent a rapid photodegradation due to the prevailing high power densities.

The requirement of transparency is accompanied by a significant loss in the value of the hyperpolarizabilty β of the molecule. Rikken and co-workers (61, 62) have investigated the conjugation dependences of molecular optical hyperpolarizabilities and found a connection between the maximum of the linear adsorption spectrum and the corresponding hyperpolarizability β. A wide range of different components was investigated, including benzene, stilbene, diphenylacetylene, various phenylvinyl heterocyclecs, oligomeric polyphenyl, α-phenylpolyene, and α, ω-diphenylpolyene, as well as other extended phenylvinyl derivatives. DC electric-field-induced second-harmonic generation (EFISH) and third-harmonic generation (THG) measurements were used for the determination of the hyperpolarizabilities. The experimental finding within a class of related derivatives could be described by power laws, i.e. $\beta \propto \lambda^4 - \lambda^9$. Hence, the requirement of blue transparency for the design of a frequency doubler of low-power diodes is accompanied by a significant loss in the hyperpolarizability. This loss in efficiency can only be counterbalanced by a long interaction length in which the fundamental and second-harmonic waves propagate with the same velocity.

2.1.4 Frequency doubler for low-power laser diodes

The design of a real device is by no means trivial since a number of performance criteria have to be fulfilled simultaneously, i.e. a high nonlinearity, transparency,

wave guide with low loss and the establishment of phase-matching conditions. Numerous materials match and optimize one property; however, the simultaneous fulfilment of all requirements still remains a challenge. Penner *et al.* (57) have reported on the fabrication of a low-loss optical waveguide fabricated by the LB technique in which precise control of the film thickness, together with inversion of the nonlinear susceptibility across the film, are used to simultaneously achieve phase-matching and improve the optical-field overlap between the propagating (fundamental and second-harmonic) waveguide modes. The resulting structure converts low-power near-infrared laser light efficiently to blue light. The performance in this case reached a practical level of performance. The assembly used is depicted in Figure 28.5. The precise control of the film thickness to a value determined by the linear optical constants enables phase-matching between the zero-order mode of the fundamental and the first-order mode of the second-harmonic wave. The modal dispersion of a waveguide allows us only to achieve phase-matching between modes of different order and not between modes of equal order. Modes of different order possess a strikingly different field distribution and this leads to a low overall efficiency due to a nearly vanishing value of the overlap integral. The latter is a peculiarity of the waveguide format and is given by the product of the field distribution of the interacting modes multiplied by the susceptibility and integrated across the cross-sectional area of the guide. Since phase matching can only be achieved between modes of different order, the resulting overlap integrals would be fairly low. However, if the sign in χ^2 is reversed at the nodal plane of the first-order mode, the overlap integral would be maximized as well. The reverse can be achieved by an upside-down orientation of the NLO active unit. Such a device has the potential to reach a practical level of performance and was able to convert low-power CW light to blue light.

In short, these papers demonstrate significant accomplishment and the viability of organic thin-film devices for nonlinear optics. They also demonstrate the possibility to tune the features of an organic molecule and establish new functions within a molecular assembly. Such devices exploit the control of the internal layer architecture on a molecularly defined level. However, despite these remarkable accomplishments the strong competition of other approaches has to be considered as well, and these alternative approaches may eventually be commercially successful. Discussions and a realistic judgement of the potential of the LB technique in this context cannot ignore the tremendous progress
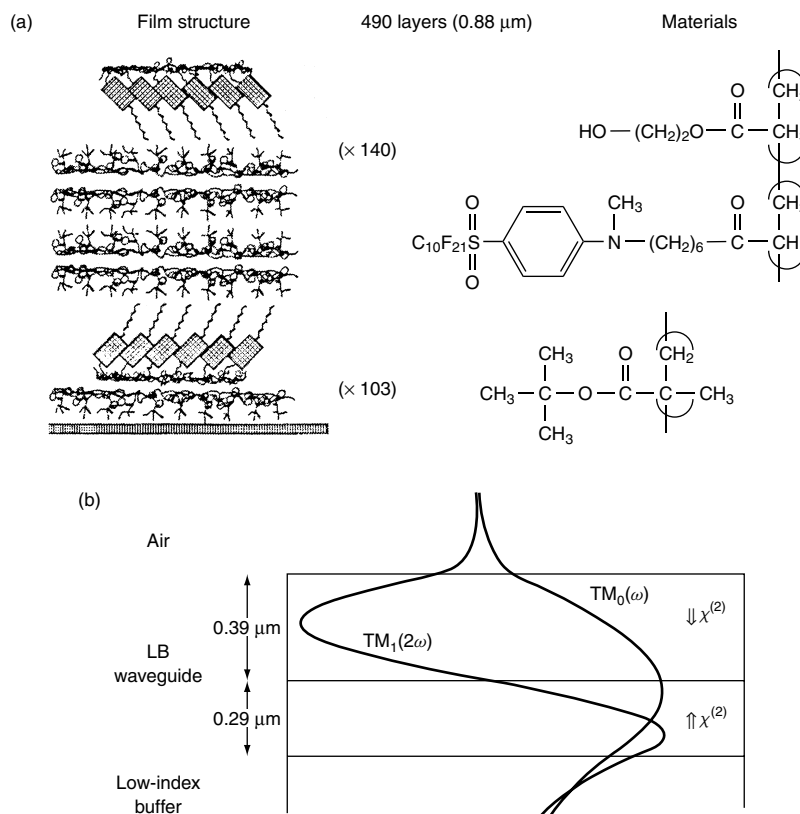
Figure 28.5. (a) Optical layer structure of the waveguide prepared by LB deposition. The thickness was adjusted to achieve phase-matching between the zero-order mode of the fundamental and the first-order mode of the generated second-harmonic by using the modal dispersion of the guide. The exact thickness is given by the linear optical constants, with only low tolerances within the nm region being acceptable. Part (b) shows the electric field distribution for the zero-order mode of the fundamental at 900 nm and the first-order mode of the second-harmonic light. The power confinement was greater than 80%. Phase-matching can only be achieved between modes of different order which limits the value of the overlap integral, where the latter is given by the product of the field distribution of the interacting modes multiplied by and the nonlinear susceptibility. A reversal of the sign of the nonlinear susceptibility at the nodal plane maximizes the value of the overlap intergral. The sign reversal was achieved by a macroscopic inverted structure. The layer architecture is schematically represented in (a), where the NLO-active unit in the upper part is invented with respect to the lower part. The performance of the system scaled up to a channel waveguide confinement is close to a practical level of performance. (From T. L. Penner, H. R. Motschmann, N. J. Armstrong, M. C. Enzenyilimba and D. J. Williams, *Nature*, **367**, 49 (1994))

of other technologies such as recent advances towards direct blue-emitting laser diodes.

2.1.5 Electro-optics

Electro-optic devices do not have the same tight tolerances as frequency doublers since they do not require phase-matching. The latter requires a careful control of the film thickness of the guide with tolerances in the nm region. All this is not required for an electro-optic modulator and opens the way for far simpler preparation techniques, such as the use of poled polymers (44). Most commonly, electro-optic modulators are based on a Mach–Zehnder interferometer in the waveguide format. The refractive index in one arm of this system is controlled by the applied electric field which slows down the propagation of light and induces a phase shift with respect to the light propagating in the other arm of the interferometer. Since modulators are operating at the frequencies used for telecommunications (1.33 or 1.5 µm), the higher values of the susceptibilities of extended π-systems can be exploited. Even though LB waveguides meet

these requirements, the lower tolerances will make this field the domain of simpler preparation techniques. The review of Ren and Dalton (64) gives a good overview on recent accomplishments. However, one should at least mention some progress with the use of LB films, such as the hybrid four-layer guide (FLG) which includes a glass guide and a 2-docosylamino-5-nitropyridine Langmuir–Blodgett film, as reported by Palchetti *et al.* (63). This device did not require a Mach–Zehnder interferometer and relied instead on guided mode interference.

2.1.6 *Promising future directions*

In the future, it will be necessary to process a steadily increasing flow of information. The processing speed of the currently used silicon technology has nearly reached the physical limit, and hence the future will demand faster alternatives such as all-optical data processing (65). The major hurdle for a realization of this vision is the design of an opto–opto switch, with the proposed device concepts exploiting third-order, $\chi^{(3)}$, nonlinear optical effects (66). The refractive index of organic materials with extended π-systems can be instantaneously changed by the exposure to light of a sufficiently high power level. The power dependence of the nonlinear refractive index can be used to control the phase of a propagating wave and is utilized in the nonlinear Mach–Zehnder interferometer as an optical switch. Suitable $\chi^{(3)}$ materials for the design of an opto–opto switch in a waveguide format have to fulfill a variety of criteria and two merit factors have been introduced, thus allowing us to judge the quality of a material and the magnitude of the achievable nonlinear phase shift (66). There have been tremendous efforts to design suitable materials and a survey and assessment can be found in the review of Luthor-Davies and Samoc (67). So far, only a few materials partially meet the requirements and none have the potential to reach a practical level of performance, which has caused some resignation within the $\chi^{(3)}$ community. In the last decade, a much more efficient way to introduce a nonlinear optical phase shift has been identified which utilizes a cascading of second-order nonlinearities (68, 69). The combination of two second-order nonlinear processes can induce a third-order nonlinearity. For instance, the combination of frequency-doubling and difference frequency mixing yields a nonlinear phase shift which is proportional to the square of the effective nonlinear susceptibility of the second order, $\chi^{(2)}$, and the same holds for a cascade of optical rectification

and the linear electro-optical effect. A good overview on the cascaded second-order nonlinear interactions can be found in the review by Bosshard (70). The concept of cascading is based on second-order effects and allows utilization of the highly developed knowledge in designing efficient $\chi^{(2)}$ materials and their structures in a new promising area. It is our belief that there is also some potential left for LB devices in such applications and that this would be a promising field for thin-film assemblies.

2.2 Sensors

Another promising application for LB films is in the field of sensors. The basic idea is simple and appealing – the Langmuir–Blodgett films are deliberately functionalized by selected moieties which specifically react to the target species, while the thin-film assemblies ensure fast response times. This specific interaction or binding change properties of the LB films are then subsequently detected and further quantified. The most simple way to monitor the binding relies on a measurement of the mass coverage at the surface via use of the quartz microbalance; however, a better sensitivity can be achieved by using optical reflection techniques, such as ellipsometry or surface plasmon spectroscopy (SPS). In the last few years, several novel detection schemes have been developed which are capable of recording a sub-monolayer coverage, as in, for instance, the heterodyne concept for the phase detection in SPS, as introduced by Nelson *et al.* (71). A discussion of various detection schemes and assessments of their sensitivities, as well as various concepts for miniaturization, is presented in the review article by Kambhampati and Knoll (72).

The design of gas sensors is meanwhile quite advanced, being driven by a growing awareness of the hazards caused by toxic or flammable gases. Safety regulations in the workplace demands an easy means to reliably detect even trace amounts of such gases. A recent review on this topic can be found in ref. (73). Many gas sensors utilize the properties of metallophthalocyanine macrocycles (74). The electronic states of such macrocycles change significantly with oxidization, with partial oxidization transforming an insulator into a conductive material. The resistance is therefore a function of the concentration of the oxidizing species, and this can be utilized for the detection of oxidizing species such as nitrogen dioxide or reducing species such as amines. The sensitivity is high and values of about 100 ppm for NO_2 or 30 ppm for NH_3 have been reported (75).

The response time and the sensitivity is linked to the order within the LB film and the use of mixtures of different materials can significantly improve the device characteristics. Emelianov and Khatko (76) have reported on an improved kinetic response and sensitivity of NO sensors based on copper tetra-*t*-butyl phthalocyanine (CuTTBPc) Langmuir–Blodgett films. The performance was greatly improved if a mixture of CuTTBPc with arachidic acid (AA) was used instead of the phthalocyanine derivative alone. De Saja *et al.* (77) have fabricated electronic sensors based on LB films of phthalocyanine derivatives which monitor volatile amines produced by the decomposition of fish and seafood. The sensor consists of an array of differently functionalized units. Each individual sensing unit undergoes changes in its electrical resistivity that are proportional to the concentration of volatile amines. The combined responses of such an array allowed an assessment of the freshness of samples of seafood.

The critical point for all of these sensors is the specificity for the target species, with different oxidizing agents, e.g. ozone, O_3, leading to similar changes. The specificity is also a critical issue for biosensors but here the "lock and key" principle of certain receptors, such as the biotin streptavidin system, can be exploited (78).

2.3   Command surfaces

Photochromic molecules have attracted a lot of research in the last few decades due to the possibility of reversibly changing their properties by the action of light (79). *Photochromism* describes the phenomenon whereby the absorption spectra of certain molecules change upon photoirradiation. Here, the exposure to light of a certain wavelength induces a new conformation or shape of the molecule, plus new physical properties. Thin-film assemblies of photochromic systems can be utilized for the design of a *command surface*, where a single monolayer of these "Smart" molecules can be sufficient to control the properties and the order in the adjacent bulk phase.

The most widely investigated photochromic system is the azobenzene chromophore (see Figure 28.6). The azobenzene possesses two distinct conformations, i.e. the (*E*)- and (*Z*)-states. Illumination of light in the near-ultraviolet region (at around 350 nm) induces an (*E*)−(*Z*) photoisomerization, while exposure to blue light reverses this isomerization. Such a reversible photoisomerization can take place with little degradation after thousands of switching cycles. The azobenzene chromophore can be incorporated in an amphiphile and processed according to the LB technique. The switching properties are maintained in the thin-film assembly provided that there is sufficient free volume. Seki and Ichimura have investigated in detail monolayer formation and LB deposition of poly(vinyl alcohol) (PVA) with an azobenzene side-chain (80). The switching efficiency in the LB films was significantly increased if the LB layer was deposited from the *cis*-state, which was explained in terms of the free volume within this layer.

These Smart surfaces can be used for controlling order in liquid crystals (LCs). Ichimura has demonstrated several light-driven liquid crystal systems, and an overview and detailed discussion is presented in a recent review article (81). The basic principle is outlined in Figure 24.6. The nematic liquid crystal is confined in a cell whose surfaces have been modified by LB films containing azobenzene units. The orientation of the nematic liquid crystal is controlled by the *cis*-/*trans*-state at the surface. The *trans*-state induces a homeotropic alignment, whereas the corresponding *cis*-state leads to a parallel alignment of the liquid crystal. It is quite remarkable that, on average, one photochromic molecule in the top-most layer is sufficient to rearrange the orientation of 10^4 LC molecules, and for this reason the terms "commander" and "soldier" molecules can properly describe such systems. The switching process is reversible and the tilt angle adopted by the LC molecules can be deliberately controlled by the (*E*)/(*Z*) ratio of the azobenzene at the surface, as monitored by waveguide spectroscopy (82). A systematic variation of the chemical structure of the command molecules and their number densities at the surface was performed by Aoki *et al.* (83) and new insights on the relevant prerequisites for an efficient photoregulation of LC orientation have been gained. The nature and the position of the substituent is decisive, with the best efficiencies being observed for *n*-alkyl chains in the *p*-position. Furthermore, it is advantageous to decouple the azobenzene from the substrate by a long spacer and adjust the number density of the azobenzene unit within certain limits. An area per azobenzene unit of $0.5-1.3$ nm^2 works best.

Möller *et al.* have used this command effect to design surfaces with a photocontrollable wetting behaviour (84). The surface of a quartz slide was modified by an azobenzene species containing fluorinated alkyl chains in the *p*-position. *Cis* and *trans* surfaces possess different wetting behaviours, which was attributed to a combination of changes in polarity and orientation order of the fluorinated substituent. It was possible to write rather fine *cis*−*trans* patterns in the surface in a reversible way and to control the formation of water droplets by light.

(a)   (b)
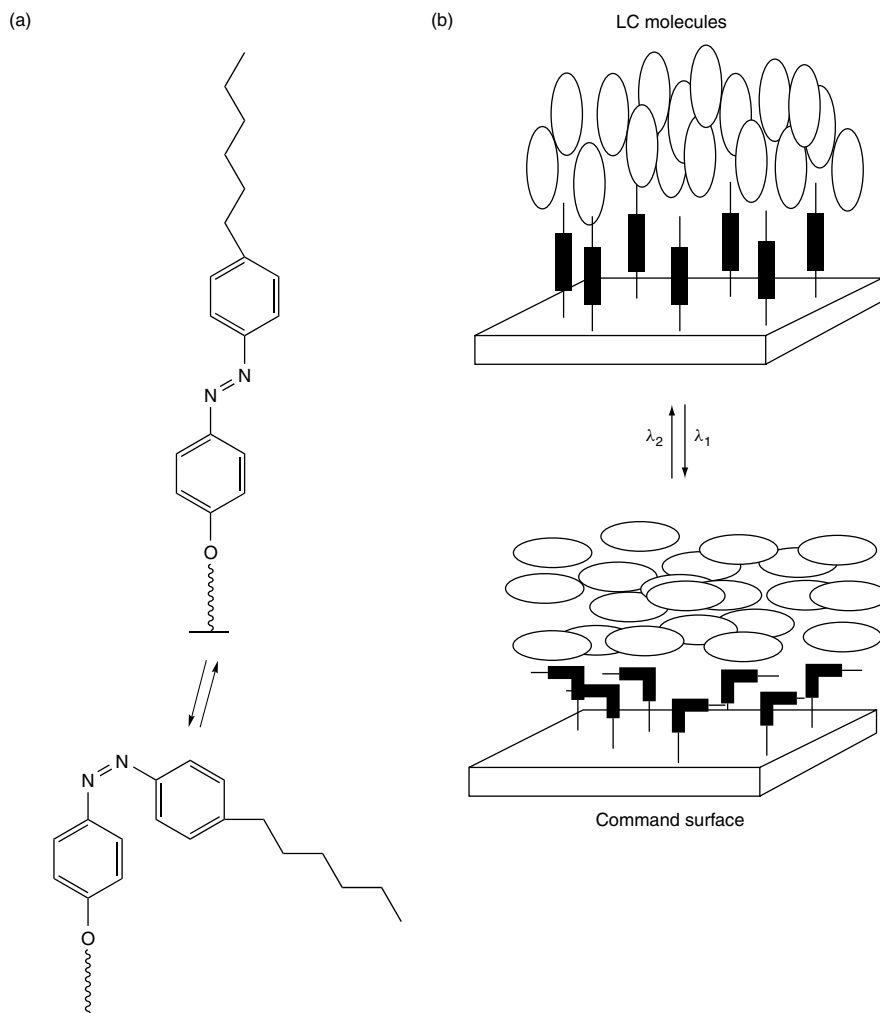
Figure 28.6. Illustration of the command effect. (a) The azobenzene possesses two distinct conformations, i.e. (E) and (Z). Illumination with UV light leads to the (Z)-state, whereas blue light switches to the (E)-state. This photochromic transition is reversible. (b) The different shapes of both states are sufficient to change the orientation of a nematic liquid crystal from an out-of-plane to an in-plane alignment. On average, one photochromic molecule at the top-most layer is sufficient to rearrange the orientation of 10^4 LC molecules. (From K. Ichimura, Supramolecular Science, 3 (1996))

Figure 24.7 shows a microscopic image of such a pattern, created by UV light and a mask. The dark areas are covered with droplets which provide the contrast in the image.

The wetting properties of structured surfaces have attracted a lot of research, both from the theoretical, as well as from the experimental point of view (85), and several wetting phases with a variety of various morphologies, such as droplets, channels or films, have been predicted. LB layers containing photochromic moieties are suitable and simple model systems for studying the scale-dependence of the predicted wetting morphologies.

2.4 Molecular electronics

One of the long-term goal of LB research defined by some groups is the field of molecular electronics with the prospect that assemblies of molecules or even individual molecules can improve certain functions required within a computer. Recent overviews on this topic can be
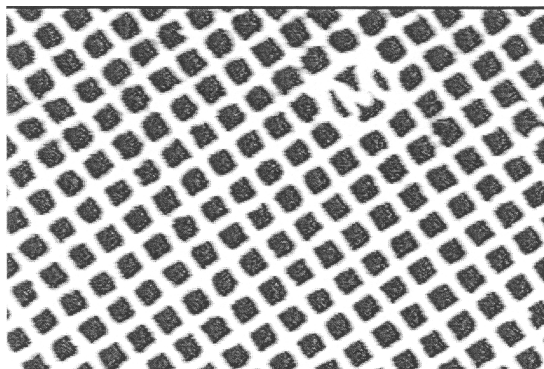
Figure 28.7. A *cis—trans* pattern was written in an LB mono-layer containing azobenzene units with fluorinated alkyl chains in the *p*-position. Both corresponding surfaces (*cis* and *trans*) differ in their wetting behaviours. Water microdroplets are formed on the illuminated regions (*cis*-state) during cooling of the sample in a humid atmosphere. The optical microscope image shows the formation of water droplet at two different stages and magnifications. The width of the bars is 2 μm and the mesh size is 10 μm. The wetting behavior can be controlled by light, and droplet formation is reversible. (From G. Möller, M. Harke, D. Prescher, H. Motschmann, Langmuir, 14, 4955, (1998))

found in the reviews by Martin and Sambles (86) and Metzger (87).
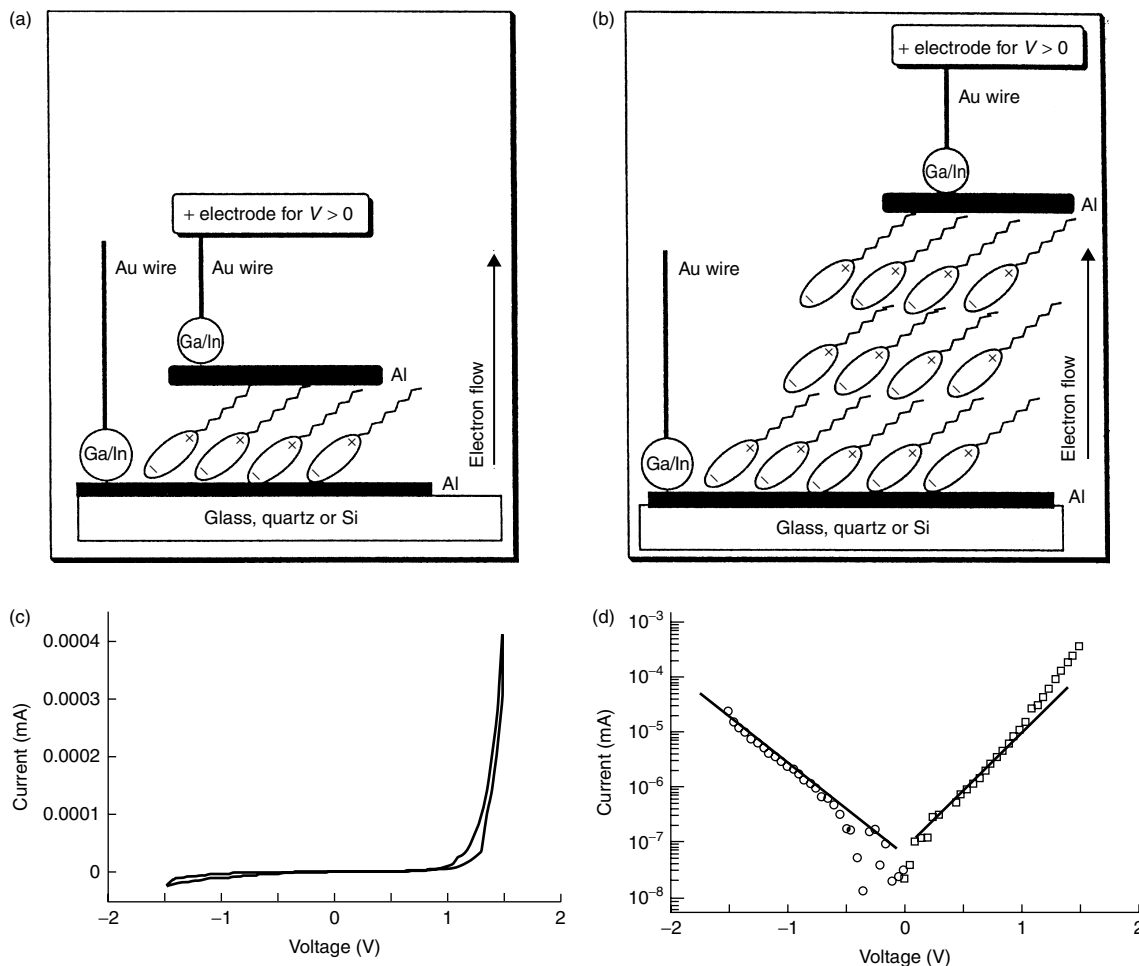
2.4.1 Molecular rectifier

Aviram and Ratner (88) proposed in the mid-1970s that a single organic molecule of the type $D-\sigma-A$, with an electron donor D and an acceptor A, separated by a σ-bond, can perform as a rectifier of electric current once properly assembled between two metal electrodes. The electronic asymmetry between the highest occupied molecular orbital (HOMO) and the lowest unoccupied molecular orbital (LUMO) of A and D should ease electron transfer from A to D and act as a high-electron-tunneling barrier in the opposite direction. Hence, an organic molecule can perform as a molecular rectifier. The proposal was made as a "Gedanken experiment" and leads to vivid research aiming for the design of suitable molecules and an experimental verification of the recti-fying properties. It is worthwhile to mention in this con-text the ongoing activities in China with the foundation of the Laboratory of Molecular and Biomolecular Elec-tronics dedicated to these topics (89) and an overview about these activities in China presented in the review by Wei (90). Meanwhile, experimental evidence has been provided that LB multilayer and monolayer can pos-sess rectifying properties (91–93). Metzger *et al*. (94)

have observed asymmetries in current—voltage measure-ments within LB monolayers in benzochalcogenazolium derivatives which possess a donor—σ—acceptor archi-tecture. The measurements were carried out on macro-scopic Al|LB|Al sandwiches, as well as via a scanning tunnelling microscopy (STM) tip. The maximum rec-tification ratio was 26:1, although a rapid degradation in performance with time was also observed. The cur-rent—voltage measurements are obtained are shown in Figure 28.8, together with a schematic of the exper-imental set-up. Brady *et al*. (95) have also reported on the rectification behaviour in $(D-\sigma-A)$ molecules. In this work, the molecules were assembled in non-centrosymmetric LB multilayer structures and sand-wiched between two metal electrodes. The electronic structure was modelled by a density-functional approach and the results were used to discuss the underlying con-duction mechanisms. Thus, about 25 years after it was first proposed, the Aviram—Ratner mechanism has been finally verified experimentally.

2.4.2 Challenges and hurdles

Can the knowledge gained in this area be further exploited for the fabrication of real devices? These present authors do not share the visions proposed for molecular electronics in the sense that individual molecules can "overtake" logic functions. The uncer-tainty principle is a good argument against overen-thusiastic proposals which may even jeopardize the credibility of this area. However, small assemblies of molecules or nanoparticles have the potential to overtake the functions required within a computer. In the follow-ing, we will outline our personal views regarding which niches, perspectives and problems we foresee in this context, plus some issues and remarks which also hold for the currently so-fashionable field of Nanoscience.

There are essentially two approaches to enter the "microworld", namely the top-down approach used by engineers and the bottom-up approach borrowed from nature. The top-down approach is based on lithography and related patterning techniques. Microstructures with function are fabricated by lithography, with a rapid trend towards smaller and smaller structures. The closest distance between adjacent electronic components within an integrated circuit (IC) defines the clock cycles and determines the speed of a processor. The current generation of chips is based on 180 nm structures which are produced by photolithography. There is a trend known as Moore's law which states that the scale of an IC halves every 18 month (96). Meanwhile, structures

Figure 28.8. Schematic representation (a) of the experimental set-up used to verify molecular rectification in a donor$-\sigma-$acceptor molecule; the electrode $(+)$ for the positive bias and the direction of an easy electron flow for $V > 0$ are marked. (b) Demonstration of rectification through a single monolayer sandwiched between Al electrodes. The DC voltage is swept at a rate of 10 mV/s and the DC current versus applied DC voltage is shown on a linear (c) and logarithmic scale (d). (From R. Metzger, B. Chen, U. Hopfner; M. Lakshmikantham, D. Vuillaume; T. Kawai, XL Wu, H. Tachibana, T. Hughes, H. Sakurai, J. W. Baldwin, C. Hosch, M. Cava, L. Brehmer, Journal of the American Chemical Society. 119(43):10455 (1997))

of about 50 nm have been successfully produced by X-ray or by electron-beam lithography, although the cost and failure rate increased tremendously, along with severe engineering problems such as capacitative coupling between components or heat dissipation (96). The top-down approach reaches physical and economic limits, and this is where the bottom-up approach may contribute as a cheap alternative.

The bottom-up approach is copied from nature and utilizes the profound knowledge gained in the self-organization of molecular assemblies and nanocrystals. Molecules and nanocrystals with different functionalities

can be designed and stacked in the desired fashion to give superlattices with novel functions. Experimental evidence has been provided that assemblies of molecules can overtake functions of the classical domain of semiconductors. However, the major challenge and hurdle for a further utilization is a combination of the macroscopic world with these nanoassemblies. A molecular assembly which overtakes the function of a transistor cannot find its place in the next generation of chips as it is not compatible with the top-down approach. This linkage between the two worlds is the major challenge. Eventually, the

bottom-up approach may provide cheap alternatives for the currently manufactured devices. However, the utilization requires a different computer architecture which takes the inherent imperfection of self-assembled structures into account. There is also research in this direction and an interesting study with an experimental computer has been performed in the laboratories of Hewlett Packard. This computer has a massively parallel architecture and was built to investigate a wide range of computational architectures and in particular address the influence of hardware defects on the overall performance (97). The machine contains over 200 000 hardware defects, and although any of these could be lethal to a conventional computer, yet it performed much faster than "high-end" single-processor workstations. The defect-tolerant architecture is due to a high communication bandwidth which enables a route around the defects. The underlying philosophy differs significantly from the usual ideas for building complex computer systems. The insight gained by these experiments may have some important implications for future computers based on any nanoassembly since the building concept of the machine takes defects into account as an inherent part of its construction (98).

3 FINAL REMARKS

LB films have been proposed for many practical applications covering a wide range of different areas from bio-sensing, to anti-reflection coatings, to all-optical processing units. Significant accomplishments in designing molecules and LB structures with functions have been made and the relationship between the macroscopic and molecular structures was in great detail addressed. Meanwhile a sound understanding of the underlying principles governing the packing and the structure of an LB film has been established. However, despite this remarkable progress, LB films have not yet found their way into the market-place and competitive approaches have been commercially more successful. Nevertheless, the LB techniques remains potentially useful due to its simplicity and the ability to build molecular assemblies defined on the molecular scale. In this respect, LB films will continue to serve as valuable model systems for addressing basic scientific problems such as wettability, friction and molecular recognition.

4 REFERENCES

1. Roberts, G., *Langmuir–Blodgett Films*, Plenum Press, New York, 1990.

2. Roberts, G. G., An applied science perspective of Langmuir–Blodgett Films, *Adv. Phys.*, **34**, 475–512 (1985).

3. Peterson, I. R., Langmuir–Blodgett techniques, in *The Molecular Electronic Handbook*, Mahler, G., May, V. and Schreiber, M. (Eds), Marcel Dekker, New York, 1994, pp. 47–77.

4. Gaines, G. L., *Insoluble Monolayers at Liquid–Gas Interfaces*, Wiley-Interscience, New York, 1966.

5. Ulmann, A., *Introduction to Ultrathin Organic Films: From Langmuir–Blodgett to Self-Assembly*, Academic Press, San Diego, CA, 1991.

6. Kaganer, M., Peterson, I. R., Kenn, R., Shih, M., Durbin, M. and Dutta, P., Tiltod phoses of fatty acid monolayers, *J. Chem. Phys.*, **102**, 9412–9422 (1995).

7. Möhwald, H., Phospholipid and phospholipid–protein monolayers at the air/water interface, *Annu. Rev. Phys. Chem.*, **41**, 441–●● (1990).

8. McConnel, H. M., Structures and transitions in lipid monolayers at the air–water interface, *Annu. Rev. Phys. Chem.*, **42**, 171–205 (1991).

9. Knobler, C. M. and Desai, R. C., Phase transition in monolayers, *Annu. Rev. Phys. Chem.*, **43**, 207–236 (1991).

10. Riviere, S., Henon, S., Meunier, J., Schwartz, D. K., Tsao, M. W. and Knobler, C. M., Texture and phase transitions in Langmuir monolayers of fatty acids – a comparative Brewster angle microscope and polarized fluorescence study, *J. Chem. Phys.*, **101**, 10045–10051 (1994).

11. Knobler, C. and Schwartz D., Langmuir and self-assembled monolayers, *Curr. Opinion Colloid Interface Sci.*, **4**, 46–51 (1999).

12. Tippmann-Krayer, P., Kenn, R. M. and Möhwald, H., Thickness and temperature dependent structure of Cd-arachidate Langmuir–Blodgett films, *Thin Solid Films*, **210/211**, 577–582 (1992).

13. Shih, M. C., Peng, J. B., Huang, K. G. and Dutta, P., Structure of fatty-acid monolayers transferred to glass substrates from various Langmuir monolayer phases, *Langmuir*, **9**, 776–778 (1993).

14. Durbin, M. K., Malik, A., Richter, A. G., Huang, K. G. and Dutta, P., *In situ* X-ray diffraction study of Langmuir–Blodgett deposition, *Langmuir*, **13**, 6547–6549 (1997).

15. Gehlert, U., Fang, J. and Knobler C., Relating the organization of the molecular tilt azimuth to lateral-force images in monolayers transferred to solid substratos, *J. Phys. Chem., B*, **102**, 2614–2617 (1998).

16. Fang, J., Gehlert, U., Shashidar, R. and Knobler, C., Imaging the azimuthal tilt order in monolayers by liquid crystal optical amplification, *Langmuir*, **15**, 297–299 (1999).

17. Spratte, K., Chi, L. and Riegler, H., Physisorption instabilities during dynamic Langmuir wetting, *Europhys. Lett.*, **25**, 211–217 (1994).

18. Spratte, K. and Riegler, H., Steady-state morphology and composition of mixed monomolecular films at the air–water interface in the vicinity of the three-phase line: Model calculations and experiments, *Langmuir*, **10**, 3161–3173 (1994).

19. Adamson, A. W., *Physical Chemistry of Surfaces*, Wiley, New York, 1993.

20. Gleiche, M. and Chi, L. F., Nanoscopic channel lattices with controlled anisotropic wetting, *Nature (London)*, **403**, 173–175 (2000).

21. Klimov, V. I., Mikhailovsky, A. A., McBranch, D. W., Leatherdale, C. A. and Bawendi, M. G., Quantization of multiparticle Auger rates in semiconductor quantum dots, *Science*, **287**, 1011–1013 (2000).

22. Murray, C. B., Kagan, C. R. and Bawendi, M. G., Self-organization of CdSe nanocrystallites into three-dimensional quantum dot superlattices, *Science*, **270**, 1335–1338 (1995).

23. Collier, B. P., Vossmeyer, T. and Heath, J. R., Nanocrystal superlattices, *Annu. Rev. Phys. Chem.*, **49**, 371–404 (1998).

24. Kotow, N., Meldrum, F., Wu, C. and Fendler, J., Mono-particulate layer and Langmuir–Blodgett type multiparticulate layers of size-quantized cadmium sulfide clusters, *J. Phys. Chem.*, **98**, 2735–2738 (1994).

25. Kotow, N., Meldrum, F., Wu, C. and Fendler, J., Mono-particulate layers of titanium dioxide nanocrystallites with controllable interparticle distances, *J. Phys. Chem.*, **98**, 8827–8830 (1994).

26. Cassagneau, T., Fendler, J. H. and Mallouk, T. E., Optical and electrical characterizations of ultrathin films self-assembled from 11-aminoundecanoic acid capped TiO2 nanoparticles and polyallylamine hydrochloride, *Langmuir*, **16**, 241–246 (2000).

27. Meldrum, F., Kotow, N. and Fendler, J., Preparation of particulate monolayers and multilayers from surfactant stabilized nanosized magnetic crystallites, *J. Phys. Chem.*, **98**, 4506–4510 (1994).

28. Meldrum, F., Kotow, N. and Fendler, J., Utilization of surfactant stabilized colloidal silver nanocrystallites in the construction of monoparticulate and multiparticulate Langmuir–Blodgett films, *Langmuir*, **10**, 2035–2040 (1994).

29. Guerin, F., Tian, Y. C. and Fendler, J. H., Dihexadecyl phosphate monolayer supported $[Ru(bpy)_{(3)}]^{(2+)}$ crystallites investigated by near-field scanning optical microscopy, *J. Phys. Chem., B*, **103**, 7882–7888 (1999).

30. Langmuir, I. and Schäfer, V., *J. Am. Chem. Soc.*, **57**, 1007–•••• (1938).

31. Heath, J. R., Knobler, C. M. and Leff, D. V., Pressure/temperature phase diagrams and superlattices of organically functionalized metal nanocrystal monolayers – the influence of particle size, size distribution, and surface passivant, *J. Phys. Chem., B*, **101**, 189–197 (1997).

32. Collier, P., Saykally, R., Shiang, J. J., Henrichs, S. E. and Heath, J. R., Reversible tuning of a silver quantum dot monolayer through the metal–insulator transition, *Science*, **277**, 1978–1979 (1997).

33. Bohren, C. F. and Huffmann, D. R., *Absorption and Scattering of Light by Small Particles*, Wiley, New York, 1983.

34. Markovich, G., Collier, C. P. and Heath, J. R., Reversible metal–insulator transition in ordered metal nanocrystal monolayers observed by impedance spectroscopy, *Phys. Rev. Lett.*, **80**, 3807–3810 (1998).

35. Kim, S. H., Medeiros-Ribeiro, G., Ohlberg, D. A. A., Williams, R. S. and Heath, J. R., Individual and collective electronic properties of Ag nanocrystals, *J. Phys. Chem., B*, **103**, 10341–10347 (1999).

36. Lefebure, S., Ménager, C., Cabuil, V., Assenheimer, M., Gallet, F. and Flament, C., Langmuir monolayers of monodispersed magnetic nanoparticles coated with a surfactant, *J. Phys. Chem., B*, **102**, 2733–2738 (1998).

37. Torimoto, T., Yamashita, M., Kuwabata, S., Sakata, T., Mori, H. and Yoneyama, H., Fabrication of CdS nanoparticle chains along DNA double strands, *J. Phys. Chem., B*, **103**, 8799–8803 (1999).

38. Schwartz, D. K., Langmuir–Blodgett film structure, *Surf. Sci. Rep.*, **27**, 241–334 (1997).

39. Kurthen, C. and Nitsch, W., Langmuir–Blodgett film of a water-soluble amphiphilic by convective monolayer compression, *Thin Solid Films*, **188**, 5–8 (1990).

40. Albrecht, O., Matsuda, H., Eguchi, K. and Nakagiri, T., Construction and use of LB deposition machines for pilot production, *Thin Solid Films*, **285**, 152–156 (1996).

41. Boyd, R. W., *Nonlinear Optics*, Academic Press, Boston, MA, 1992.

42. Shen, R., *Principles of Nonlinear Optics*, Wiley, New York, 1984.

43. Koechner, W., *Solid State Laser Engineering*, Springer-Verlag, 1992.

44. Prasad, P. and Williams, D. J., *Introduction to Nonlinear Optical Effects in Molecules and Polymers*, Wiley, New York, 1991.

45. Cai, C. Z., Liakatas, I., Wong, M. S., Bosch, M., Bosshard, C., Gunter, P., Concilio, S., Tirelli, N. and Suter, U. W., Donor-acceptor-substituted phenylethenyl bithiophenes: Highly efficient and stable nonlinear optical chromophores, *Org. Lett.*, **1**, 1847–1849 (1999).

46. Marder, S. R., Kippelen, B., Jen, A. K. -Y. and Peyghambarian, N., Design and synthesis of chromophors and polymers for electrooptic and photorefractive applications, *Nature (London)*, **388**, 845–851 (1997).

47. Williams, D. J., Organic polymeric and non-polymeric materials with large optical nonlinearities, *Angew. Chem. Int. Ed. Engl.*, **23**, 690–697 (1984).

48. Schrader, S., Zauls, V., Dietzel, B., Flueraru, C., Prescher, D., Reiche, J., Motschmann, H. and Brehmer, L., Linear and nonlinear optical properties of Langmuir–Blodgett multilayers from chromophore-containing maleic acid anhydride polymers, *Mater. Sci. Eng. C*, **8–9**, 527–537 (1999).

49. Ashwell, G. J., Zhou, D. J. and Skjonnemand, K., Z-type films of a two-legged optically nonlinear dye, *Mol. Cryst. Liq. Cryst., Sect. A*, **337**, 413–416 (1999).

50. Ashwell, G. J., Zhou, D. J. and Huang, C. H., Z-type Langmuir–Blodgett films of a three-component optically nonlinear dye, *Colloids Surf., A*, **155**, 47–50 (1999).

51. Ashwell, G. J., Handa, T. and Ranjan, R., Improved second-harmonic generation from homomolecular Langmuir–Blodgett films of a transparent dye, *J. Opt. Soc. Am., B*, **15**, 466–470 (1998).

52. Zhou, D. J., Ashwell, G. J. and Huang, C. H., Improved second-harmonic generation from Langmuir–Blodgett monolayers of an ionically combined bis-chromophore zinc complex, *Chem. Lett.*, 7–8 (1997).

53. Ashwell, G. J., Walker, T. W., Leeson, P., Grummt, U. W. and Lehmann, F., Improved second-harmonic generation from Langmuir–Blodgett films, *Langmuir*, **14**, 1525–1527 (1998).

54. Motschmann, H., Penner, T., Armstrong, N. and Enzenyilimba, M., Additive second-order nonlinear susceptibilities in Langmuir–Blodgett multibilayers: testing the oriented gas model, *J. Phys. Chem.*, **97**, 3933–3936 (1993).

55. Wijekoon, W. M. K. P., Wijaya, S. K., Bhawalkar, J. D., Prasad, P. N., Penner, T. L., Armstrong, N. J., Enzenyilimba, M. C. and Williams, D. J., Second harmonic generation in multilayer Langmuir–Blodgett films of blue transparent organic polymers, *J. Am. Chem. Soc.*, **118**, 4480–4483 (1996).

56. Verbiest, T., Elshocht, S. V., Kauranen, M., Hellemans, L., Snauwaert, J., Nuckolls, C., Katz, T. and Persoons, A., Strong enhancement of nonlinear optical properties through supramolecular chirality, *Science*, **282**, 913–915 (1998).

57. Penner, T. L., Motschmann, H. R., Armstrong, N. J., Enzenyilimba, M. C. and Williams, D. J., Efficient phase-matched second-harmonic generation of blue light in an organic waveguide, *Nature (London)*, **367**, 49–51 (1994).

58. Dalton, L. R., Polymeric electro-optic modulators. from chromophore design to integration with semiconductor and silica fiber optics, *Ind. Eng. Chem. Res.*, **38**, 8–33 (1999).

59. Kalluri, S., Ziari, M., Chen, A., Chuyanov, V., Steier, W. H., Chen, D., Jatali, D., Fettermann, H. R. and Dalton, L. R., Monolithic integration of waveguide polmer electrooptic modulators on VLSI circuits, *IEE Photon. Tech. Lett.*, **8**, 644–646 (1996).

60. Cheng, D., Fettermann, H. R., Steier, W. H., Dalton, L. R., Weng, W. and Shi, Y., Demonstration of a 110 GHz electrooptic polymer modulator, *Appl. Phys. Lett.*, **70**, 2082–2084 (1997).

61. Cheng, L. -T., Tam, W., Marder, S. R., Stiegman, A. E., Rikken, G. and Spangler, C. W., Experimental investigations of organic molecular nonlinear optical polarizabilities. II. A study of conjugation dependences, *J. Phys. Chem.*, **95**, 10643–10652 (1991).

62. Cheng, L. -T., Tam, W., Stevenson, S. H., Meredith, G. R., Rikken, G. and Marder, S. R., Experimental investigations of organic molecular nonlinear optical polarizabilities. I. Methods and results on benzene and stilbene derivatives, *J. Phys. Chem.*, **95**, 10631–10643 (1991).

63. Palchetti, L., Sottini, S., Grando, D., Giorgetti, E., Ricceri, R. and Gabrielli, G. I., Electrooptic modulation of laser diode light by mode interference in a multilayer waveguide including a 2-docosylamino-5-nitropyridine Langmuir–Blodgett film, *Appl. Phys. Lett.*, **72**, 873–875 (1998).

64. Ren, A. and Dalton, L. R., Electroactive polymers, including nonlinear optical polymers, *Curr. Opinion Colloid Interface Sci.*, **4**, 165–171 (1999).

65. Halvorson, C. and Heeger, A. J., Two photon absorption and ultrafast optical computing, *Synth. Met.*, **71**, 1649–1652 (1995).

66. Stegeman, G. and Torruellas, W., Nonlinear materials for information processing and communications, *Philos. Trans. R. Soc. Lond., Phys. Sci. Eng.*, **354**, 754–756 (1996).

67. Luther-Davies, B. and Samoc, M., Third-order nonlinear optical organic materials for photonic switching, *Curr. Opinion Solid State Mater. Sci.*, **2**, 213–219 (1997).

68. Wang, Z., Hagan, D., VanStryland, E., Zyss, J., Vidakovik, P. and Torruellas, W., Cascaded second-order effects in *N*-4-nitrophenyl-L-prolinol in a molecular single crystal, *J. Opt. Soc. Am., B*, **14**, 76–86 (1997).

69. Baek, Y., Schiek, R., Stegeman, G., Krijnen, G., Baumann, I. and Sohler, W., All-optical integrated Mach-Zehnder switching due to cascaded nonlinearities, *Appl. Phys. Lett.*, **68**, 2055–2057 (1996).

70. Bosshard, C., Cascading of second-order nonlinearities in polar materials, *Adv. Mater.*, **8**, 385–392 (1996).

71. Nelson, S. G., Johnston, K. S. and Yee, S. S., High sensitivity surface plasmon resonance sensor based on phase detection, *Sensors Actuators, B*, **35/36**, 187–199 (1996).

72. Kambhampati, D. and Knoll, W., Surface plasmon optics, *Curr. Opinion Colloid Interface Sci.*, **4**, 273–280 (1999).

73. Guillaud, G., Simon, J. and Germain, J. P., Metallophthalocyanines – gas sensors, resistors and field effect transistors, *Coord. Chem. Rev.*, **180**(2), 1433–1484 (1998).

74. Leznoff, C. C. and Lever, A. B., *Phthalocyanines, Properties and Applications*, Vols 1–4, VCH, New York, 1989–1996.

75. Arnold, D. P., Manno, D., Micocci, G., Serra, A., Tepore, A. and Valli, L., Porphyrin dimers linked by a conjugated alkyne bridge – novel moieties for the growth of Langmuir–Blodgett films and their applications in gas sensors, *Langmuir*, **13**, 5951–5956 (1997).

76. Emelianov, I. L. and Khatko, V. V., Gas sensing properties of the composite Langmuir–Blodgett films: effects of the film thickness and the Cd^{2+} addition into the subphase, *Sensors Actuators, B*, **60**, 221–227 (1999).

77. de Saja, R., Souto, J., Rodriguez-Mendez, M. L. and de Saja, J. A., Array of lutetium bis-phthalocyanine sensors for the detection of trimethylamine, *Mater. Sci. Eng., C*, **8–9**, 565–568 (1999).

78. Zislperger, M. and Knoll, M., Multispot parallel online monitoring of interfacial binding reactions by surface plasmon microscopy, *Prog. Colloid Polym. Sci.*, **109**, 244–253 (1998).

79. Dürr, H. and Laurent, B., *Photochromism: Molecules and Systems*, Elsevier, Amsterdam, 1991.

80. Seki, T. and Ichimura, K., Formation and Langmuir–Blodgett deposition of monolayers of poly(vinyl alcohol) having azobenzene side-chains, *Polym. Commun.*, **30**, 108–110 (1989).

81. Ichimura, K., Surface-assisted photoregulation of molecular assemblages as commander/soldier molecular systems, *Supramol. Sci.*, **3**, 67–73 (1996).

82. Knobloch, H., Orendi, H., Büchel, M., Seki, T., Ito, S. and Knoll, W., Photochromic command surface induced

switching of liquid crystal optical waveguide structures, *J. Appl. Phys.*, **77**, 481–487 (1995).

83. Aoki, K., Seki, T., Suzuki, Y., Tamaki, T., Hosoki, A. and Ichimura, K., Factors affecting photoinduced alignment regulation of nematic liquid crystals by azobenzene molecular films, *Langmuir* **8**, 1007–1013 (1992).

84. Möller, G., Harke, M., Prescher, D. and Motschmann, H., Controlling microdroplet formation by light, *Langmuir*, **14**, 4955–4958 (1998).

85. Lipowsky, R., Lenz, P. and Swain, P. S., Wetting and dewetting of structured and imprinted surfaces, *Colloids Surfaces, A*, **161**, 3–22 (2000).

86. Martin, A. S. and Sambles, J. R., Molecular rectification, photodiodes and symmetry, *Nanotechnology*, **7**, 401–405 (1996).

87. Metzger, R. M., Electrical rectification by a molecule: The advent of unimolecular electronic devices, *Acc. Chem. Res.*, **32**, 950–957 (1999).

88. Aviram, A. and Ranter, M., *Chem. Phys. Lett.*, **29**, 277–283 (1974).

89. Wei, Y., Lu, Z., Yuan, C. and Gan, Q., Molecular electronics: strategies and progress in China, *IEEE Eng. Med. Biol.*, **16**, 53–61 (1997).

90. Wei, Y., Molecular electronics – the future of bioelectronics, *Supramol. Sci.*, **5**, 723–731 (1998).

91. Polymeropolos, E., Möbius, D. and Kuhn, H., Molecular assemblies with functional units of sensitizing and conducting molecular components: photovoltage, dark conduction and photoconduction, *Thin Solid Films*, **68**, 173–179 (1980).

92. Geddes, N. J., Sambles, J. R., Jarvis, D., Parker, W. and Sandman, D. J., Fabrication and investigation of asymmetric current voltage characteristics of a metal/Langmuir–Blodgett/metal structure, *Appl. Phys. Lett.*, **56**, 1916–1919 (1990).

93. Ashwell, G. J., Sambles, J. R., Martin, A. S., Parker, W. G. and Slablewski, M., Rectifying characteristics of Mg/$C_{16}H_{33}-Q_3C$ LB films/Pt structures, *J. Chem. Soc., Chem. Comm.*, 1374–1376 (1990).

94. Metzger, R. M., Chen, B., Hopfner, U., Lakshmikantham, M., Vuillaume, D., Kawai, T., Wu, X. L., Tachibana, H., Hughes, T., Sakurai, H., Baldwin, J. W., Hosch, C., Cava, M. and Brehmer, L., Unimolecular electrical rectification in hexadecylquinolinium tricyanoquinodimethanide, *J. Am. Chem. Soc.*, **119**, 10455–10466 (1997).

95. Brady, A. C., Hodder, B., Martin, A. S., Sambles, J. R., Ewels, C. P., Jones, R., Briddon, P. R., Musa, A. M., Panetta, C. A. F. and Mattern, D. L., Molecular rectification with M vertical bar(D–sigma–A LB film) vertical bar M junctions, *J. Mater. Chem.*, **9**, 2271–2275 (1999).

96. Schaller, R. R., Moore's law: past, present and future, *IEEE Spectrum*, **34**(6) 52–56 (1997).

97. Clark, D., TERAMAC – pointing the way to real-world nanotechnology, *IEEE Comput. Sci. Eng.*, **5**, 88–90 (1998).

98. Heath, J., Kuekes, P., Snider, G. and Williams, R., A defect tolerant computer architecture: opportunities for nanotechnology, *Science*, **280**, 1716–1721 (1998).